Density functional study of 1,3,5-trinitro-1,3,5-triazine molecular crystal with van der Waals interactions

Fuyuki Shimojo,[1,2,a)] Zhongqing Wu,[1] Aiichiro Nakano,[1,a)] Rajiv K. Kalia,[1] and Priya Vashishta[1]

[1]*Department of Computer Science, Department of Physics and Astronomy, and Department of Chemical Engineering and Materials Science, Collaboratory for Advanced Computing and Simulations, University of Southern California, Los Angeles, California 90089-0242, USA*
[2]*Department of Physics, Kumamoto University, Kumamoto 860-5555, Japan*

Volume dependence of the total energy and vibrational properties of crystalline l,3,5-trinitro-l,3,5-triazine (RDX) are calculated using the density functional theory (DFT). For this molecular crystal, properties calculated with a generalized gradient approximation to the exchange-correlation energy differ drastically from experimental values. This discrepancy arises from the inadequacy in treating weak van der Waals (vdW) interactions between molecules in the crystal, and an empirical vdW correction to DFT (DFT-D approach by Grimme) is shown to account for the dispersion effects accurately for the RDX crystal, while incurring little computational overhead. The nonempirical van der Waals density-functional (vdW-DF) method also provides an accurate description of the vdW corrections but with orders-of-magnitude more computation. We find that the vibrational properties of RDX are affected in a nontrivial manner by the vdW correction due to its dual role—reduction of the equilibrium volume and additional atomic forces. © *2010 American Institute of Physics*. [doi:10.1063/1.3336452]

The nitramine, hexahydro-1,3,5-trinitro-1,3,5-triazine (RDX) ($C_3N_6O_6H_6$), is an important energetic material used as propellants and explosives. Though RDX releases a large amount of energy in its bulk form,[1] even higher energy density is achieved by forming nanocomposite materials,[2–4] in which RDX encapsulates nanoscale reactant particles such as highly combustive Al particles.[5,6] In order to design more efficient and insensitive energetic materials,[7–10] it is important to establish a reliable theoretical method that describes mechanical properties of condensed phases of RDX correctly.

Theoretical investigations of RDX molecules are divided into two categories: Those based on analytic interatomic potentials[11–15] and others based on nonempirical electronic structure calculations[16–23] using the density functional theory (DFT) or Hartree–Fock (HF) method. In the former, the parameters in the interatomic potentials are determined empirically[11,12,15] or derived from nonempirical calculations.[13,14] Since the parameter fitting always includes crystal data (even when fitted to nonempirical data), the potentials describe crystal properties at ambient conditions rather accurately with lattice constants within 2%–4% errors[11,13,15] and the bulk modulus within the experimental accuracy.[12,13] These potentials have been used successfully in molecular-dynamics simulations to study, e.g., planar shock propagation in an RDX crystal prior to detonation.[14,15]

Nonempirical electronic-structure calculations often have significant errors in crystal properties of RDX[20–22] and other energetic molecular crystals[24–27] at ambient conditions.

It is well known that the generalized gradient approximation (GGA) to the exchange-correlation energy in DFT tends to overestimate crystal volumes, while the local density approximation (LDA) underestimates them. It was reported that GGA and LDA give 7%–30% larger and 10%–15% smaller volumes, respectively, for RDX,[20–22] CL-20,[20,21] HMX,[20,21] TATB,[21,25] PETN,[21,27] TNAD,[24] and FOX-7,[26] compared to experimental values. Also, the bulk moduli calculated by GGA and LDA are often significantly smaller and larger, respectively, than experimental values.[26] These errors are commonly attributed to the inadequacy of the current DFT in treating weak van der Waals interactions between molecules, which are expected to play a significant role in determining the mechanical properties of these molecular crystals. The importance of the dispersion component of van der Waals interactions for RDX has been pointed out in recent theoretical studies.[28–30] They used a symmetry-adapted perturbation theory based on DFT description of monomers [SAPT(DFT)] to describe the weak interactions between RDX molecules, thereby successfully reproducing the crystal structures.

In the present study, crystal properties of RDX are calculated in the framework of DFT with van der Waals corrections. We test two approaches: (1) the DFT-D method by Grimme,[31,32] which is an empirical correction to DFT for taking into account the dispersive interactions based on damped, atomic-pairwise potentials, and (2) the van der Waals density functional (vdW-DF)[33,34] with a nonlocal correlation energy expressed in terms of a density-density interaction formula, among several alternatives[35,36] to incorporate van der Waals interactions into DFT. Both approaches have been successfully applied to weakly interacting molecular

a)Authors to whom correspondence should be addressed. Electronic addresses: shimojo@kumamoto-u.ac.jp and anakano@usc.edu.
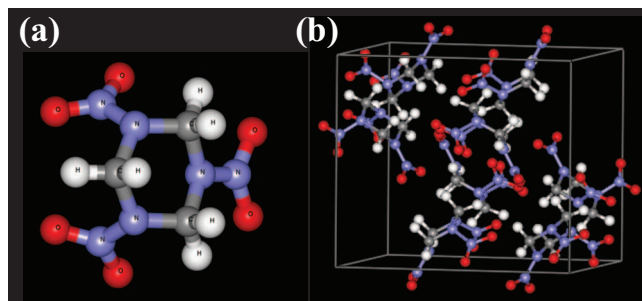
FIG. 1. (a) An RDX molecule with carbon (gray), hydrogen (white), oxygen (red), and nitrogen (blue) atoms. (b) The unit cell of an RDX crystal containing eight RDX molecules.
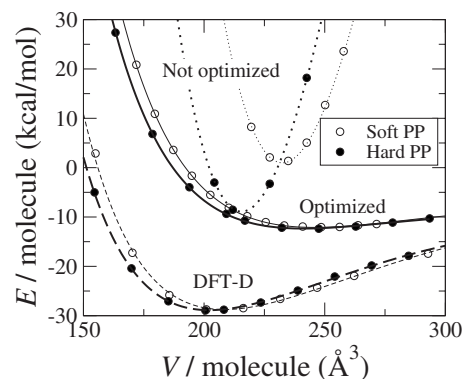

FIG. 2. Total energy of RDX crystal as a function of volume. The open and solid circles show the results obtained by soft-PP and hard-PP, respectively. The curves represent the fitting to Murnaghan equation of state (Ref. 43). The dotted and solid curves correspond to the DFT calculations within GGA with the PBE functional, without and with the optimization of atomic positions, respectively. The dashed curves are the total energy obtained by DFT-D. The origin of energy is taken to be the energy of an isolated molecule.

systems as well as rare gases, whereas their applicability to a molecular crystal is examined here.

Before applying the dispersive corrections, we first calculate the lattice parameters of the RDX crystal by GGA with the Perdew–Burke–Erzerhof (PBE) functional.[37] The electronic wave functions and the electron density are expanded in plane-wave basis sets. The energy functional is minimized iteratively using a preconditioned conjugate-gradient method.[38,39] Two sets of ultrasoft pseudopotentials[40] are used to calculate the crystal properties. The first set, hereafter referred to as "soft PP," is constructed from larger cutoff radii r_{cl} (l is the angular-momentum quantum number), beyond which the pseudowave functions coincide with the all-electron wave functions. The second set, hereafter referred to as "hard PP," is generated from smaller cutoff radii r_{cl}. The plane-wave cutoff energies for the electronic pseudowave functions and the pseudocharge density are 30 and 200 Ry, respectively, for soft-PP, and 45 and 250 Ry, respectively, for hard-PP, which give a convergence of the total energy within 0.5 mRy/electron. See supplemental material[41] for more information on these pseudopotentials.

As shown in Fig. 1, each RDX molecule ($C_3H_6N_6O_6$) consists of 21 atoms, and 8 RDX molecules (i.e., 168 atoms) are contained in the unit cell of the RDX crystal, which is orthorhombic with the experimental lattice constants of a =13.182, b=11.574, and c=10.709 Å.[42] The electronic-structure calculations are carried out for the unit cell under periodic boundary conditions in all directions. The Γ point is used for Brillouin zone sampling, because the lattice parameters are known to change only by 1.4% when four k points are used.[20]

We first calculate the lattice constants of the RDX crystal, which minimize the total energy, using experimental atomic coordinates without relaxation of atomic positions. The optimized values (percent errors in parentheses) are a =13.78 Å (4.5%), b=12.11 Å (4.6%), and c=11.18 Å (4.4%) for soft-PP, and a=13.45 Å (2.0%), b=11.81 Å (2.0%), and c=10.88 Å (1.6%) for hard-PP. The calculated results are unexpectedly in good agreement with experiments. The errors for hard-PP are smaller than those for soft-PP, which is the same trend as observed for diatomic molecules. These results seem to indicate that PBE-GGA gives the lattice constants of RDX with reasonable accuracy, contrary to previous studies.[20–27] It was reported that the HF approximation also gives rather good lattice constants when

atomic coordinates are not relaxed.[16] These agreements, however, are fortuitous, and when the atomic coordinates are fully relaxed, PBE-GGA exhibits serious problems in reproducing the crystal properties. In the relaxation calculations, the unit cell is constrained to be orthorhombic, and the RDX molecules are relaxed without any other constraints. The optimized lattice parameters are a=14.13 Å (7.2%), b =12.35 Å (6.7%), and c=11.51 Å (7.4%) for soft-PP, and a=13.94 Å (5.6%), b=12.23 Å (5.7%), and c=11.35 Å (5.6%) for hard-PP. Here, the errors for both sets of pseudopotentials are similarly large. These values are consistent with those obtained by the previous studies.[20,21] Although we do not restrict crystal symmetry in the structural relaxation, the space group Pbca is well preserved. Even when the atomic structure is relaxed with the crystal symmetry, the optimized lattice parameters change within 1% compared to those without constraints.

To study the volume dependence of the total energy, we minimize the enthalpy at a given pressure with respect to the orthorhombic lattice vectors. The ratios between the lattice parameters have rather weak pressure dependence, and the orthorhombic cell changes almost uniformly up to 10 GPa (see the supplemental material).[41] Figure 2 shows the total energy as a function of volume, where the circles are the calculated values and the curves are fitted to the Murnaghan equation of state.[43] Solid and dotted curves are obtained by the PBE-GGA calculations with and without the optimization atomic coordinates, respectively. Table I shows the equilibrium volume V_0 and the bulk modulus B obtained from the fitting. The lattice energy U_0 (the energy required to separate the lattice into isolated molecules) at equilibrium is also listed. It is observed that the PBE-GGA calculation without the optimization of the atomic coordinates gives a very large B and a very small or negative U_0. On the other hand, when the atomic coordinates are optimized, the calculated B is reduced to almost half the experimental value for both soft-PP and hard-PP, and V_0 becomes too large (by 20%) compared to the experimental value. U_0 is still too small, compared to the heat of sublimation (31.11 kcal/mol) observed experi-

TABLE I. Equilibrium volume V_0 and bulk modulus B, obtained from the fitting to Murnaghan equation of state (Ref. 43), and lattice energy U_0 at equilibrium.

Method	V_0 (Å^3)		B (GPa)		U_0 (kcal/mol)	
	Soft-PP	Hard-PP	Soft-PP	Hard-PP	Soft-PP	Hard-PP
PBE-GGA						
No structural relaxation	233.2	216.0	131.1	130.3	−0.9	8.9
With structural relaxation	250.9	241.9	6.7	6.1	12.1	12.3
DFT-D						
With structural relaxation	211.3	202.1	11.4	11.3	28.8	28.9
Experiments	204.2[a]		11–13[b]		31.11[c]	

[a]Reference 42.
[b]Reference 13.
[c]Reference 44 (heat of sublimation).

mentally. The PBE-GGA is thus unable to describe the elastic and cohesive properties of the RDX crystal satisfactorily.

We next apply van der Waals corrections to the PBE-GGA calculations discussed above. The DFT-D method proposed by Grimme[31,32] includes an empirical van der Waals correction to standard density functional, where the total energy is given by

$$E_{\text{DFT-D}} = E_{\text{KS-DFT}} + E_{\text{disp}}, \tag{1}$$

where $E_{\text{KS-DFT}}$ is the usual self-consistent Kohn–Sham energy as obtained from the density functional of choice and E_{disp} is an empirical dispersion correction given by

$$E_{\text{disp}} = -s_6 \sum_{i<j} \frac{C_{ij}}{R_{ij}^6} f_{\text{damp}}(R_{ij}). \tag{2}$$

Here, C_{ij} denotes the dispersion coefficient for the pair of ith and jth atoms, s_6 is a global scaling factor that only depends on the density functional used, and R_{ij} is an interatomic distance. A damping function f_{damp} is introduced to avoid near singularities for small R_{ij}. Grimme determined necessary parameters for the elements H–Xe for several common density functionals including PBE.[31,32] The DFT-D method has been applied to several molecular systems, which have weak noncovalent interactions, and the results demonstrate that dispersion effects are important in such systems.[45] The semiempirical van der Waals correction has also been applied to periodic solids,[46,47] such as crystalline CH_4, layered graphite and V_2O_5 structures, and rare-gas solids. However, we are unaware of DFT-D calculations of energetic molecular crystals, such as RDX, which contain hundreds of atoms per unit cell.

The optimized lattice parameters for RDX crystal obtained using the DFT-D method are $a=13.40$ Å (1.7%), $b=11.50$ Å (−0.6%), and $c=10.97$ Å (2.4%) for soft-PP, and $a=13.20$ Å (0.1%), $b=11.45$ Å (−1.0%), and $c=10.71$ Å (−0.0%) for hard-PP. The agreement with the experimental values is quite well. The energy-volume curves are displayed by the dashed curves in Fig. 2. The corresponding V_0 and B are listed in Table I. The discrepancy between the calculated and experimental V_0 is reduced significantly from ~20% for PBE-GGA to less than 1% for DFT-D. Furthermore, B is obtained within the experimental accuracy with DFT-D, and U_0 becomes comparable to the heat of sublimation. These results demonstrate the adequacy of the DFT-D method to account for the dispersion effects in RDX molecular crystal at ambient conditions. It should also be noted that the empirical correction, Eqs. (1) and (2), is easy to add into an existing DFT program and incurs little computational overhead. Here, it should be noted that the experimental values were obtained at room temperature. The temperature effects have been studied in recent calculations based on the SAPT-(DFT) approach,[28–30] which have shown that the volume expands ~3% at room temperature compared to the 0 K value (as compared to the van der Waals correction on the volume, which is ~20%).

Finally, we test another van der Waals density functional (vdW-DF)[33,34] with a nonlocal correlation energy. The exchange-correlation energy in vdW-DF is given by

$$E_{\text{xc}} = E_{\text{x}}^{\text{revPBE}} + E_{\text{c}}^{\text{LDA}} + E_{\text{c}}^{\text{nl}}, \tag{3}$$

where $E_{\text{x}}^{\text{revPBE}}$ and $E_{\text{c}}^{\text{LDA}}$ are simply the revPBE-exchange[33] and LDA-correlation functionals, respectively. The third term represents a fully nonlocal correlation functional given by

$$E_{\text{c}}^{\text{nl}} = \frac{1}{2} \int_{\text{cell}} d\mathbf{r} \int_{\text{all space}} d\mathbf{r}' \, n(\mathbf{r}) \phi(\mathbf{r}, \mathbf{r}') n(\mathbf{r}'), \tag{4}$$

where $n(\mathbf{r})$ is the electron density and the kernel $\phi(\mathbf{r}, \mathbf{r}')$ is a function of $n(\mathbf{r})$, $n(\mathbf{r}')$, their gradients, and $\mathbf{r} - \mathbf{r}'$.[33,48] It has been shown that vdW-DF appropriately describes dispersion interactions within weakly interacting molecular systems.[49–51] We implemented the exchange-correlation potential[34] for the vdW-DF functional in our program to carry out fully self-consistent calculations. However, this requires massive computation to evaluate the double integral in Eq. (4) using the fast-Fourier-transform (FFT) grid points, especially for large supercells. In the case of the RDX crystalline unit cell, direct calculation of the double integral is prohibitive because the total number of grid points exceeds 1×10^6, and some simplifications are needed. Although the $\mathbf{r}'$ integral in Eq. (4) extends formally over the entire space, it can be carried out practically within a spatial subregion provided it is sufficiently large. We perform the $\mathbf{r}'$ integral within a sphere of radius R around each $\mathbf{r}$. In addition, the $\mathbf{r}$ and $\mathbf{r}'$ integrals are sampled on every other point of the FFT
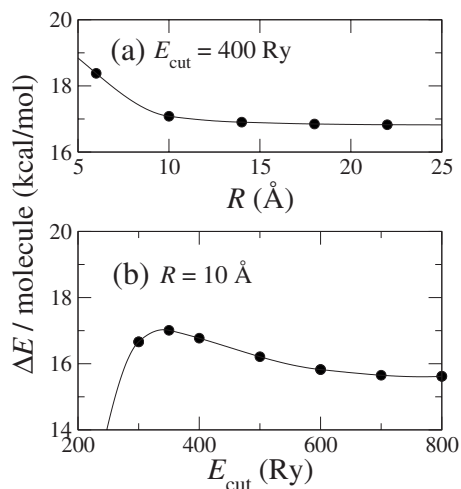
FIG. 3. Total energy difference $\Delta E = E(V_1) - E(V_2)$ as a function of (a) the integration radius R of the second integral in Eq. (4), and (b) the plane-wave cutoff energy E_{cut} for the electron density. $E(V)$ is the total energy of RDX crystal with volume V obtained by vdW-DF with soft-PP. V_1 and V_2 are 173.5 and 204.1 Å^3/molecule, respectively. The R dependence is calculated with $E_{cut} = 400$ Ry, and the E_{cut} dependence is obtained with $R = 10$ Å.

grid as suggested previously.[49] To validate these simplifications, we confirmed that the interaction energy of an Ar dimer is correctly reproduced as described in the supplemental material.[41]

We apply the validated calculation procedure above to the RDX crystal with soft-PP. Before the energy-volume curve is examined, we investigate the dependence of the total energy on the integration radius R of the $\mathbf{r}'$ integral in Eq. (4) as well as on the size of the FFT grid. The latter is characterized by the plane-wave cutoff energy E_{cut} for the electron density $n(\mathbf{r})$. In the calculations with soft-PP, the cutoff energy $E_{cut} = 200$ Ry is large enough to expand $n(\mathbf{r})$. It is, however, not obvious whether the corresponding FFT grid is small enough to calculate the double integral in Eq. (4), because the integrand includes the product of $n(\mathbf{r})$, which means that a finer grid might be needed. Also, we use only every other point of the FFT grid for the numerical integration, and therefore it is necessary to see how the calculated results depend on the size of the grid. Figures 3(a) and 3(b) show the R and E_{cut} dependence, respectively, of the total energy difference $\Delta E = E(V_1) - E(V_2)$, where $E(V)$ is the total energy of RDX crystal with volume V, and $V_1 = 173.5$ and $V_2 = 204.1$ Å^3/molecule. The atomic structure for each volume is optimized within vdW-DF with $R = 10$ Å and $E_{cut} = 200$ Ry. The rapid convergence of ΔE with R in Fig. 3(a) indicates that the elastic properties as a function of volume can be described accurately even when the total energy is not fully converged. Specifically, the energy difference between $V = 173.5$ and 204.1 Å^3/molecule converges within 0.3 kcal/mol at $R = 10$ Å. We observe that the total energy is more sensitive to E_{cut} than to R. Nevertheless, the E_{cut} dependence of ΔE in Fig. 3(b) again shows good convergence as in the case of R. The energy difference between $V = 173.5$ and 204.1 Å^3/molecule at $E_{cut} = 400$ Ry is 17.0 kcal/mol, which is only 1.5 kcal/mol larger than that at $E_{cut} = 800$ Ry.

Figure 4 shows the energy-volume curve obtained by vdW-DF with $R = 10$ Å and $E_{cut} = 400$ Ry, which is com-
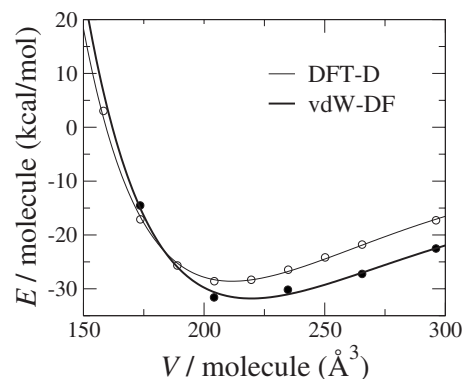

FIG. 4. Total energy of RDX crystal as a function of volume obtained by vdW-DF (thick line) and DFT-D (thin line) with soft-PP. The origin of energy is taken to be the energy of an isolated molecule.

pared with the results of the DFT-D method with soft-PP. Although the electronic structures are calculated self-consistently within vdW-DF, the atomic positions and the lattice parameters are not optimized here because of the high computational cost of vdW-DF. (Note that the atomic positions are optimized by vdW-DF with $R = 10$ Å and $E_{cut} = 200$ Ry as described above.) From this curve, we see that the current vdW-DF calculations give $V_0 = 223.3$ Å^3/molecule, $B = 10.4$ GPa, and $U_0 = 31.8$ kcal/mol, which are in reasonable agreement with the experimental results. Note that the total energy by vdW-DF converges within 0.3 kcal/mol with respect to R at $R = 10$ Å and within 1.5 kcal/mol with respect to E_{cut} at $E_{cut} = 400$ Å as shown in Fig. 3. The accuracy of the calculated results may be improved by using larger values of R and E_{cut} and with further structural optimization.

As shown in Fig. 4, both DFT-D and vdW-DF treat van der Waals corrections accurately in DFT calculations for RDX crystal. While the computational costs of the DFT-D method are essentially the same as the conventional DFT method (i.e., the calculations of the DFT-D corrections are negligible), the vdW-DF method needs a large amount of computations as described in the supplemental material.[41] Note that an implementation of the vdW-DF method has been proposed[52] recently to reduce the computational cost, though its applicability to RDX is yet to be tested.

In order to demonstrate the applicability of the DFT-D method, we calculate vibrational properties of the RDX crystal using the density functional perturbation theory.[53,54] The results are summarized in Tables II and III, where both the results with and without the vdW correction by DFT-D are shown, which are abbreviated to "PBE-D" and "PBE," respectively, in the tables. In the orthorhombic unit cell with space group Pbca, there are eight RDX molecules (see Fig. 1). Each molecule has 21 atoms and hence has 57 internal modes. Each internal mode is split into eight modes in the crystal because of the vibrational coupling effect between molecules (splitting effect). However, since the interactions between the RDX molecules are very weak, the splitting effect is negligible for most of the internal modes, and the split in the frequency is typically less than 1 cm^{-1}. The calculated frequencies listed in Table II are the averages over eight split

TABLE II. Internal vibrational modes of RDX under ambient pressure.

	Frequency (cm^{-1})						
	This work		calc.[a]	calc.[b]			Vibration assignment[e]	Molecular symmetry
	(PBE-D)	(PBE)	(PW91)	(B3LYP)	exp.[c]	exp.[d]		
1	3107	3106	3141	3206	3076	3075	CH st	A′
2	3102	3100	3136	3199	3067	3067	CH st	A″
3	3091	3090	3125	3205			CH st	A″
4	3021	3007	3043	3081	3003	3001	CH st	A′
5	2963	2956	2998	3016	2949	2949	CH st	A′
6	2953	2947	2984	3015	2906		CH st	A″
7	1566	1567	1601	1668	1595	1593	O–N–O st	A′
8	1543	1545	1580	1648	1573	1570	O–N–O st	A″
9	1498	1505	1551	1623	1542	1538	O–N–O st.	A″
10	1423	1427	1448	1496	1508	1508	N–N st+CH$_2$ sci	A′
11	1402	1408	1422	1480	1460	1456	N–N st+CH$_2$ sci	A′
12	1387	1392	1409	1468	1436	1433	CH$_2$ sci	A″
13	1357	1353	1385	1420	1422	1422	N–N st+CH$_2$ sci	A′
14	1347	1343	1353	1406	1388	1387	N–N st+CH$_2$ wag	A″
15	1328	1318	1335	1374	1377	1377	N–N st+CH$_2$ wag	A′
16	1314	1313	1322	1362	1351	1346	CH$_2$ tw+CNC st	A″
17	1304	1300	1312	1362	1309	1309	CH$_2$ tw+N–N st	A′
18	1285	1279	1306	1299			CH$_2$ wag+ring tw {rot}	A″
19	1239	1234	1287	1337	1273	1273	CH$_2$ wag+N–N st	A′
20	1234	1230	1255	1270	1273		CH$_2$ wag+N–N st	A″
21	1219	1211	1222	1296	1249		CNC st	A′
22	1209	1209	1226	1264	1249		CNC st	A′
23	1206	1207	1215	1238	1232	1232	CNC st+CH$_2$ tw	A″
24	1189	1186	1210	1230	1215	1214	CNC st+N–N st	A′
25	1103	1108	1112	1153	1031	1029	ring	A″
26	1003	993	1058	1036	1023		CNC st+N–N st+ONO st	A′
27	986	984	997	1011	945	943	CH$_2$ r+CN st+N–N st	A″
28	923	919	935	951	920	920	CH$_2$ r+ring b+N–N st	A′
29	894	891	916	937	885	884	CH$_2$ r+CN st+N–N st	A′
30	872	868	886	909	858	855	CN st+N–N st	A″
31	858	860	868	896	848	847	ring CNC st+NO$_2$ sci	A′
32	831	831	835	870			ring CNC st+NO$_2$ sci	A″
33	823	822	827	855	788	786	ring CNC st+NO$_2$ sci	A′
34	757	755	760	803	757	756	ring NCN sci+NO$_2$ sci	A′
35	726	725	725	769	739	739	N NO$_2$ u	A′
36	722	722	721	761			N NO$_2$ u	A″
37	706	709	711	756			N NO$_2$ u	A′
38	654	650	659	676	670	669	ring b+NO$_2$ sci	A′
39	624	623	635	651	607	605	ring tw+NO$_2$ sci	A″
40	587	580	593	610	590	589	ring tw+NO$_2$ r	A′
41	576	572	583	588	588		ring tw {rot}+NO$_2$ r	A″
42	568	563	577	579	488	486	ring tw+NO$_2$ r	A″
43	459	448	455	463	464	463	ring b {folding}	A′
44	439	412	416	438	429		ring b {fatterning}	A′
45	404	393	399	403	415		NNC$_2$ u	A″
46	397	383	393	406	364	414	NNC$_2$ u+NO$_2$ r	A′
47	358	348	355	371	347	347	ring tw	A″
48	340	328	338	325	301		ring st	A′
49	294	286	302	290	226	224	ring tw {rot}+NO$_2$ r	A″
50	223	210	226	209	207	205	NNC$_2$ u+NO$_2$ r	A″
51	206	191	217	229			NNC$_2$ u+NO$_2$ r	A′
52	162	132	178	107	149		NO$_2$ rot	A″
53	147	122	171	93	131		NO$_2$ rot	A′

TABLE II.   (*Continued.*)

	Frequency (cm⁻¹)					Vibration assignment[e]	Molecular symmetry
	This work		calc.[a]	calc.[b]			
	(PBE-D)	(PBE)	(PW91)	(B3LYP)	exp.[c]	exp.[d]	
54	131	109	158	74			NO_2 rot	A''
55	121	96	144	63	107	106	NO_2 wag+lattice	A''
56	106	86	123	60			NO_2 wag+lattice	A''
57	96	79	116	44	90	90	NO_2 wag+lattice	A'

[a]PW91 calculations for the crystal (Ref. 22).
[b]B3LYP calculations for a single molecule (Ref. 17).
[c]Raman experiments for the crystal (Ref. 55).
[d]Raman experiments for the crystal (Ref. 56).
[e]Abbreviations: (st) stretch, (tw) twist, (sci) scissor, (r) rock, (b) bend, (u) umbrella, (rot) rotation, and (wag) wagging.

modes corresponding to respective internal modes. The remaining 48 modes are lattice modes, where the entire RDX molecule vibrates almost like a rigid body. Half of these lattice modes have the inversion symmetry and hence are Raman active. They are listed in Table III.

The calculated frequencies of the internal modes are compared with previous calculations for the crystal[22] and a single molecule[17] as well as to Raman spectroscopy data[55,56] in Table II. Except for the six lowest frequencies, the frequencies for a single molecule are larger than those for the crystal. This difference results from the crystal field effects due to the structural difference between a single molecule and molecules in the bulk crystal. The frequencies based on this calculation agree generally well with those from the previous crystal calculation[22] and with the Raman spectroscopy data.[55,56] The vdW correction significantly increases the six

TABLE III. Lattice modes of RDX under ambient pressure.

Mode	Symmetry	Frequency (cm⁻¹)		calc.[a]	exp.[b]	exp.[c]
		This work				
		(PBE-D)	(PBE)			
		(Translational modes)				
L_6	A_g	92.8	71.9	98	70	69, 72, 76
	B_{1g}	89.1	66.9	91	70	
	B_{2g}	82.3	66.2	98	74	
	B_{3g}	85.3	68.2	100	70	
L_5	A_g	84.5	60.2	88	59	60
	B_{1g}	74.1	59.0	80	59	
	B_{2g}	74.3	56.8	85	60	
	B_{3g}	79.7	64.0	77	59	
L_4	A_g	72.0	56.4	73	51	46, 51
	B_{1g}	69.3	53.3	68	52	
	B_{2g}	67.8	51.2	74	49	
	B_{3g}	71.5	53.7	66	49	
		(Librational modes)				
L_3	A_g	63.4	49.2	60	51	
	B_{1g}	56.6	43.2	56	46	
	B_{2g}	54.6	46.0	54		
	B_{3g}	58.3	41.3	53	49	
L_2	A_g	43.1	33.8	52	33	29, 38
	B_{1g}	34.5	25.5	48	28	
	B_{2g}	34.6	31.7	28	29	
	B_{3g}	45.8	35.1	41	37	
L_1	A_g	9.6	7.6	32	20	21
	B_{1g}	−8.7	−8.4	−38	20	
	B_{2g}	−21.9	−23.3	−30	20	
	B_{3g}	−23.1	−46.8	−25	19	

[a]Reference 22.
[b]Reference 57.
[c]Reference 55.

lowest frequencies, because these modes are sensitive to small changes of intermolecular distance.

As listed in Table III, the frequencies of the lattice modes obtained by the present calculation with the vdW correction are smaller or comparable with those by the previous calculation,[22] even though the volume of the crystal in the previous calculation is significantly larger. The frequencies calculated without the vdW correction are about 30% smaller than those with the vdW correction. Both present and previous calculations are in agreement with Raman measurements.[55,57]

There are two distinct effects of the vdW correction on the vibration properties. One arises from the equilibrium-volume decrease due to the vdW correction, and the other originates from the additional atomic forces obtained by the gradient of Eq. (2). While the latter affects the phonon frequencies only within a few cm^{-1}, the former effect is significant when the vdW correction decreases the equilibrium volume largely as in the case of RDX. As shown in Table I, DFT-D decreases the optimized volume by about 14%. Therefore, the frequencies of lattice modes are increased by about 30% due to the vdW correction (Table III). On the other hand, the effects on internal modes are insignificant except for few low frequency modes (Table II). This is because the bond lengths within the molecules are almost unchanged by the vdW correction, while the intermolecular distances are reduced considerably.

In summary, we performed electronic structure calculations of the RDX molecular crystal based on DFT. The crystal properties obtained by using PBE-GGA differ drastically from experimental values. This failure of PBE-GGA has been shown to arise from the inadequacy in treating weak van der Waals interactions between molecules. The empirical DFT-D method has been shown to produce crystal properties in good agreement with the experiments. We also tested a nonempirical vdW-DF approach to treat van der Waals interactions. Although the calculated total energy is not fully converged with parameters for computations, the energy-volume curve is obtained with reasonable accuracy. In conclusion, DFT-D is accurate enough to practically describe dispersion effects in molecular crystals such as RDX with little computational overhead, whereas vdW-DF is potentially more accurate but is highly time consuming to be applied to large systems. Calculation of the vibrational properties using the DFT-D method revealed a dual role of the vdW correction.

ACKNOWLEDGMENTS

[1] R. A. Fifer, in *Fundamentals of Solid-Propellant Combustion*, edited by K. K. Kuo and M. Summerfield (AIAA Inc., New York, 1984), Vol. 90.

[2] Y. Q. Yang, Z. Y. Sun, S. F. Wang, and D. D. Dlott, J. Phys. Chem. B **107**, 4485 (2003).

[3] Y. Q. Yang, S. F. Wang, Z. Y. Sun, and D. D. Dlott, Appl. Phys. Lett. **85**, 1493 (2004).

[4] R. J. Jouet, A. D. Warren, D. M. Rosenberg, V. J. Bellitto, K. Park, and M. R. Zachariah, Chem. Mater. **17**, 2987 (2005).

[5] N. E. Schultz, G. Staszewska, P. Staszewski, and D. G. Truhlar, J. Phys. Chem. B **108**, 4850 (2004).

[6] N. E. Schultz and D. G. Truhlar, J. Chem. Theory Comput. **1**, 41 (2005).

[7] R. A. Yetter, F. L. Dryer, M. T. Allen, and J. L. Gatto, J. Propul. Power **11**, 683 (1995).

[8] W. H. Wilson, M. P. Kramer, and R. W. Armstrong, Abstr. Pap.-Am. Chem. Soc. **221**, U608 (2001).

[9] M. M. Hurley, C. F. Chabalowski, G. H. Lushington, and D. Sorescu, Abstr. Pap.-Am. Chem. Soc. **220**, U284 (2000).

[10] K. L. McNesby, A. W. Miziolek, T. Nguyen, F. C. Delucia, R. R. Skaggs, and T. A. Litzinger, Combust. Flame **142**, 413 (2005).

[11] D. C. Sorescu, B. M. Rice, and D. L. Thompson, J. Phys. Chem. B **101**, 798 (1997).

[12] T. D. Sewell and C. M. Bennett, J. Appl. Phys. **88**, 88 (2000).

[13] A. Strachan, E. M. Kober, A. C. T. van Duin, J. Oxgaard, and W. A. Goddard, J. Chem. Phys. **122**, 054502 (2005).

[14] K. I. Nomura, R. K. Kalia, A. Nakano, P. Vashishta, A. C. T. van Duin, and W. A. Goddard, Phys. Rev. Lett. **99**, 148303 (2007).

[15] M. J. Cawkwell, T. D. Sewell, L. Q. Zheng, and D. L. Thompson, Phys. Rev. B **78**, 014107 (2008).

[16] A. B. Kunz, Phys. Rev. B **53**, 9733 (1996).

[17] B. M. Rice and C. F. Chabalowski, J. Phys. Chem. A **101**, 8720 (1997).

[18] D. Chakraborty, R. P. Muller, S. Dasgupta, and W. A. Goddard, J. Phys. Chem. A **104**, 2261 (2000).

[19] W. F. Perger, R. Pandey, M. A. Blanco, and J. J. Zhao, Chem. Phys. Lett. **388**, 175 (2004).

[20] E. F. C. Byrd, G. E. Scuseria, and C. F. Chabalowski, J. Phys. Chem. B **108**, 13100 (2004).

[21] E. F. C. Byrd and B. M. Rice, J. Phys. Chem. C **111**, 2787 (2007).

[22] M. S. Miao, Z. A. Dreger, J. M. Winey, and Y. M. Gupta, J. Phys. Chem. A **112**, 12228 (2008).

[23] N. Umezawa, R. K. Kalia, A. Nakano, P. Vashista, and F. Shimojo, J. Chem. Phys. **126**, 234702 (2007).

[24] L. Qiu, H. M. Xiao, W. H. Zhu, J. J. Xiao, and W. Zhu, J. Phys. Chem. B **110**, 10651 (2006).

[25] H. Liu, J. J. Zhao, J. G. Du, Z. Z. Gong, G. F. Ji, and D. Q. Wei, Phys. Lett. A **367**, 383 (2007).

[26] J. J. Zhao and H. Liu, Comput. Mater. Sci. **42**, 698 (2008).

[27] M. W. Conroy, I. I. Oleynik II, S. V. Zybin, and C. T. White, Phys. Rev. B **77**, 094107 (2008).

[28] R. Podeszwa, R. Bukowski, B. M. Rice, and K. Szalewicz, Phys. Chem. Chem. Phys. **9**, 5561 (2007).

[29] R. Podeszwa, B. M. Rice, and K. Szalewicz, Phys. Rev. Lett. **101**, 115503 (2008).

[30] R. Podeszwa, B. M. Rice, and K. Szalewicz, Phys. Chem. Chem. Phys. **11**, 5512 (2009).

[31] S. Grimme, J. Comput. Chem. **25**, 1463 (2004).

[32] S. Grimme, J. Comput. Chem. **27**, 1787 (2006).

[33] M. Dion, H. Rydberg, E. Schroder, D. C. Langreth, and B. I. Lundqvist, Phys. Rev. Lett. **92**, 246401 (2004).

[34] T. Thonhauser, V. R. Cooper, S. Li, A. Puzder, P. Hyldgaard, and D. C. Langreth, Phys. Rev. B **76**, 125112 (2007).

[35] P. L. Silvestrelli, Phys. Rev. Lett. **100**, 053002 (2008).

[36] A. Tkatchenko and M. Scheffler, Phys. Rev. Lett. **102**, 073005 (2009).

[37] J. P. Perdew, K. Burke, and M. Ernzerhof, Phys. Rev. Lett. **77**, 3865 (1996).

[38] G. Kresse and J. Hafner, Phys. Rev. B **49**, 14251 (1994).

[39] F. Shimojo, R. K. Kalia, A. Nakano, and P. Vashishta, Comput. Phys. Commun. **140**, 303 (2001).

[40] D. Vanderbilt, Phys. Rev. B **41**, 7892 (1990).

[41] See supplementary material at http://dx.doi.org/10.1063/1.3336452 for details of pseudopotentials, the volume change of lattice parameters, and complementary description of the vdW-DF method.

[42] C. S. Choi and E. Prince, Acta Crystallogr., Sect. B: Struct. Crystallogr. Cryst. Chem. **28**, 2857 (1972).

[43] F. D. Murnaghan, Proc. Natl. Acad. Sci. U.S.A. **30**, 244 (1944).

[44] J. M. Rosen and C. Dickinso, J. Chem. Eng. Data **14**, 120 (1969).

[45] S. Grimme, J. Antony, T. Schwabe, and C. Muck-Lichtenfeld, Org. Bio-

mol. Chem. **5**, 741 (2007).

[46] F. Ortmann, F. Bechstedt, and W. G. Schmidt, Phys. Rev. B **73**, 205101 (2006).

[47] T. Kerber, M. Sierka, and J. Sauer, J. Comput. Chem. **29**, 2088 (2008).

[48] M. Dion, H. Rydberg, E. Schroder, D. C. Langreth, and B. I. Lundqvist, Phys. Rev. Lett. **95**, 109902 (2005).

[49] A. Puzder, M. Dion, and D. C. Langreth, J. Chem. Phys. **124**, 164105 (2006).

[50] J. Kleis, B. I. Lundqvist, D. C. Langreth, and E. Schroder, Phys. Rev. B **76**, 100201 (2007).

[51] V. R. Cooper, T. Thonhauser, and D. C. Langreth, J. Chem. Phys. **128**, 204102 (2008).

[52] G. Román-Pérez and J. M. Soler, Phys. Rev. Lett. **103**, 096102 (2009).

[53] S. Baroni, S. de Gironcoli, A. Dal Corso, and P. Giannozzi, Rev. Mod. Phys. **73**, 515 (2001).

[54] P. Giannozzi, S. Baroni, N. Bonini, M. Calandra, R. Car, C. Cavazzoni, D. Ceresoli, G. L. Chiarotti, M. Cococcioni, I. Dabo, A. Dal Corso, S. de Gironcoli, S. Fabris, G. Fratesi, R. Gebauer, U. Gerstmann, C. Gougoussis, A. Kokalj, M. Lazzeri, L. Martin-Samos, N. Marzari, F. Mauri, R. Mazzarello, S. Paolini, A. Pasquarello, L. Paulatto, C. Sbraccia, S. Scandolo, G. Sclauzero, A. P. Seitsonen, A. Smogunov, P. Umari and R. M. Wentzcovitch, J. Phys: Condes. Matter **21**, 395502 (2009).

[55] Z. A. Dreger and Y. M. Gupta, J. Phys. Chem. B **111**, 3893 (2007).

[56] M. Rey-Lafon, C. Trinquecoste, R. Cavagnat, and M.-T. Forel, J. Chim. Phys. Phys.-Chim. Biol. **68**, 1533 (1971).

[57] M. Rey-Lafon, R. Cavagnat, C. Trinquecoste, and M.-T. Forel, J. Chim. Phys. Phys.-Chim. Biol. **68**, 1573 (1971).